Engineering Failure Analysis 118 (2020) 104787

Contents lists available at ScienceDirect

Engineering Failure Analysis

journal homepage: www.elsevier.com/locate/engfailanal

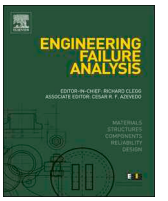

A probabilistic study of welding residual stresses distribution and their contribution to the fatigue life

Asma Manai[a,*], Rüdiger Ulrich Franz von Bock und Polach[b], Mohammad Al-Emrani[a]

[a] Chalmers University of Technology, Department of Architect and Civil Engineering, 41296 Gothenburg, Sweden
[b] Hamburg University of Technology (TUHH), Ship Structural Design and Analysis, 21073 Hamburg, Germany

ARTICLE INFO

Keywords:
Welding
Residual stresses shapes
Probability density function
Compressive residual stresses
Tensile residual stresses

ABSTRACT

Welding is a joining process that is associated with heating cycles which leads to considerable change in local material microstructure and the formation of high welding Residual stresses (RS) in the welded joint. Residual stresses can have a detrimental effect on the fatigue strength of welded joints. In this paper, previously published data from measurements of residual stresses in various types of welded joints are compiled. In total, more than 100 test results are studied covering steels with yield strengths between 307 MPa and 1050 MPa in different welded details (butt joints, longitudinal and transverse attachments, cruciform joints, as well as K-joints) with varying thicknesses.

The collected data is used to study the distribution of welding residual stresses (regardless of the welding parameters) at weld toe and through the thickness of the welded plate. Probabilistic analysis is then used to arrive at a model that represents the value and distribution of residual stresses in welded joints. This model is used to predict and explain the scatter in fatigue test data from recent fatigue testing of welded samples.

1. Introduction

Welding of metals was introduced in the late 1930s and the early 1940s with the purpose of replacing riveted and bolted joints. Since then, new welding technologies have been developed such as metal inert gas (MIG), metal active gas (MAG) welding [2] and lately laser welding [1]. Welding is a heat-intensive process that changes local material properties (microstructure, hardness, yield strength, etc.) and introduces weld defects, stress concentration and Residual Stresses (RS), which are detrimental for the fatigue performance of welded structures.

Nasir et al. [3] showed that weld effects (changes in the material properties and microstructures as well as residual stresses) are highly dependent on the method of welding and welding parameters, such as current and voltage, wire size and wire feeding speed, welding speed as well as the choice of shielding gas and gas flow rate [2]. The chemical composition of the steel and matching of weld and base metal properties [4–7] are also important parameters in controlling weld quality and welding residual stresses as well as the resultant weld geometry, e.g. weld angle and weld toe radius. In their study, Naser et al. [3] are limited to study the welded parameters without investigating how these parameters will affect the magnitude and the depth of the residual stresses.

To answer the challenge which is “determination of welding RS distribution”, many models [8,9,10,11] have been developed based on finite element analysis using different welding parameters. However, numerical simulation of welding processes is a complex and time-consuming task that requires extensive and accurate input to provide reliable results. As a deduction from [8–11],

* Corresponding author.
E-mail address: asma.manai@chalmers.se (A. Manai).

https://doi.org/10.1016/j.engfailanal.2020.104787
Received 13 November 2019; Received in revised form 12 July 2020; Accepted 4 August 2020
Available online 18 August 2020
1350-6307/ © 2020 Elsevier Ltd. All rights reserved.

Nomenclature

RS	residual stresses
RS_A	magnitude of residual stresses at the surface, (at point A)
$RS_{A'}$	magnitude of residual stresses at the sub-surface with the same sign as point A, (at point A′)
RS_B	magnitude residual stresses at the sub-surface, (at point B)
f_y	yield strength of the material
α	Constant $\frac{RS_A}{f_y}$
β	Constant $\frac{RS_B}{f_y}$
γ	Constant $\frac{RS_{A'}}{f_y}$
$D_{A'}$	depth of the $RS_{A'}$
D_B	depth of the RS_B
σ_u	ultimate strength
x	no value
RV	random variable
N_A	number of cycles to introduce damage = 1 at point A
N_B	number of cycles to introduce damage = 1 at point B
$\sigma_{a,ext}$	external stress range
$\sigma_{m,ext}$	external mean stress
k_t	stress concentration factor
k_f	effective notch factor
$\sigma_{res,x}$	residual stresses in the x-direction
$\sigma_{res,y}$	residual stresses in the y-direction
σ_a	stress amplitude

it is impossible to have sufficient details of all the welding processes to do such a simulation with satisfying accuracy in results. Furthermore, these models are very sensitive to the provided welding parameters, a small change in one value of these parameters changes the welding residual stresses distribution significantly.

Therefore, in the design phase, it is often assumed that RS from welding (regardless of the welding parameters) is in the order of magnitude of the material yield strength and that these stresses are tensile in fatigue critical locations (weld toe, for example). The method used in engineering is an empirical method overestimating the residual stresses distribution affecting the designed fatigue life of structures.

None of these sources [3,8,9,10,11] present a clear and straight forward method predicting a reliable welding residual stresses distribution through the thickness without being costly with respect to resources and time. Even for the work that measured RS distribution in the thickness direction, they are limited to present the measured results without any interpretation of the measured data. In real civil or mechanical structures, it is possible to measure the surface residual stresses, but it is very challenging to measure the residual stresses distribution through the thickness.

For the welded components, serious fatigue problems were reported right from the beginning of the service life. Radaj [12] reviewed the state of the art of fatigue properties of welded joints produced by a different welding process. The author concluded that residual stresses, stress concentration at weld toe and weld defects are the governing parameters responsible for higher or lower fatigue life in comparison to the base metal. Therefore, the effect of residual stresses should be introduced in the calculation of crack initiation and the weldment fatigue life.

The present investigation aims to predict, regardless of the welding parameters, a reliable shape of the welding residual stresses distribution at the weld toe through the plate thickness. In addition to that, within this paper, the contribution of welding RS to the crack initiation and the fatigue life prediction was performed.

The present paper starts with Section 2 where the fundamental aspect of residual stresses was presented. In Section 3, a probabilistic analysis of the collected published data of welding RS distribution is performed. A method to determine the shape welding residual stresses at the weld toe through the thickness direction is developed. In Section 4, an experimental study is carried-out first,

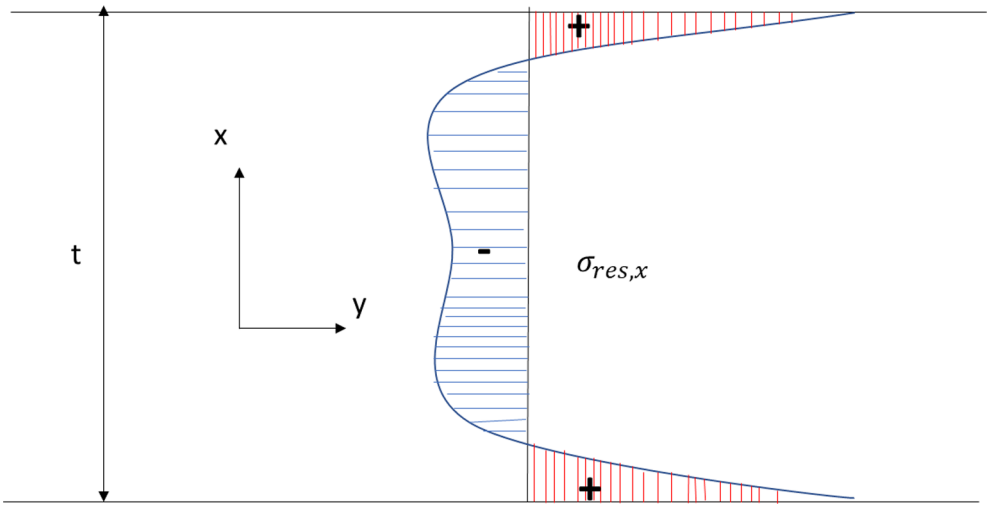

Fig. 1. Schematic distribution of residual stresses [13].

to evaluate the proposed method and second, to investigate the effects of welding residual stresses on the fatigue life through a redraw of the S-N curve condescending RS of welded steel transversal joint S355.

2. Residual stresses

By definition, residual stresses refer to a self-balancing state of stress which can be present in structures without any external load [13], see Fig. 1. The equilibrium of the self-balanced stress can be translated to:

Equilibrium in x-direction gives

$$\int_{-t/2}^{t/2} \sigma_{res,x} dy = 0 \tag{1}$$

The absence of external moment translated to the following equation

$$\int_{-t/2}^{t/2} y\sigma_{res,x} dy = 0 \tag{2}$$

where 't' is the plate thickness and, $\sigma_{res,x}$ is the residual stresses in the x-direction.

Residual stresses present results of such process as manufacturing, welding, surface treatment, assembling, Heat treatment, etc. As these processes are uncertain, they lead to introduce uncontrolled RS.

Residual stresses from welding can be measured by means of several methods. X-ray and neutron diffraction are two non-destructive methods that can give a view of the surface and the shallow sub-surface residual stresses. The former can also be used to measure the distribution of RS below the surface (i.e. through the thickness) by successively removing surface layers in small increments, for example by means of chemical etching. The method of hole-drilling is an old and well-established destructive technique for measuring sub-surface residual stresses distribution. Detailed information about X-Ray, Neutron diffraction and hole drilling can be found in [14].

In this paper, a focus is put on welding residual stresses distribution along the thickness direction at the weld toe.

3. Method

In this wide literature study measurements, data of residual stresses are collected. However, most of them are limited to giving only the magnitude of the measured surface residual stresses. Only 29 measurements provided information about the distribution of RS through plate thickness. As the objective of the current work is to study the distribution of residual stresses through the thickness of welded joints, only measurements that provided such information are used in the evaluation.

Based on Section 2, providing only the magnitude of surface RS (magnitude of residual stresses at the surface) an infinite number of solutions satisfy Eqs. (1) and (2). In light of this, additional variables are required to identify a unique solution that represents the physical distribution of the residual stresses through the thickness direction. Hence, for a welded detail constructed with any material and plate thickness, knowing the magnitude and the depth of the maximum sub-surface RS (see Fig. 2) in addition to the magnitude of the surface RS is sufficient to find the unique solution for the distribution of residual stresses through plate thickness. In that, it is, of course, assumed that a linear distribution of residual stresses is a sufficiently good approximation or idealization with respect to the aim of this study.

A review of the collected measurement data shows that in most cases measured residual stresses on the surface were tensile,

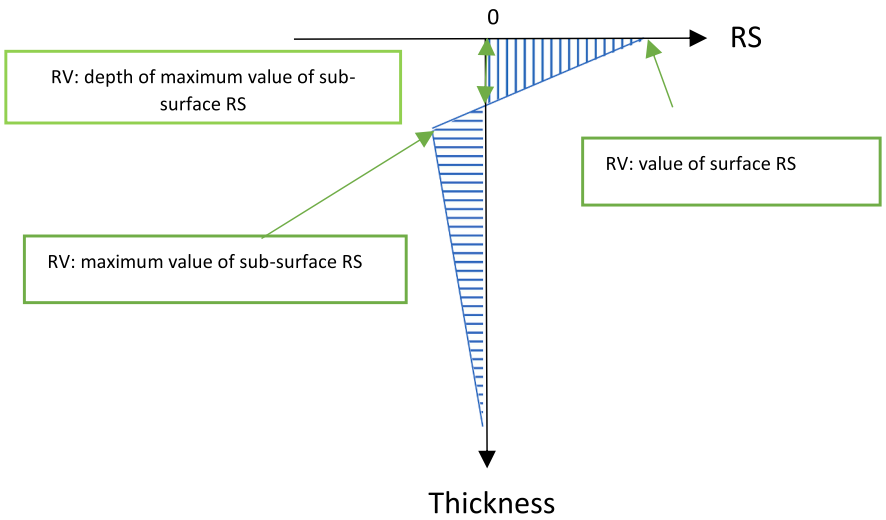

Fig. 2. RS distributions (shape) along the thickness direction.

balanced by compressive stresses below the surface. This is what is usually assumed in welded connections. There are however still a considerable amount of measurements [30–36] that confirmed an opposite distribution, i.e. compressive stresses at the surface balanced by tensile sub-surface stresses. Therefore, in analyzing uncertainties in the distribution of welding residual stresses, both cases have to be considered.

As the measuring of residual stresses along thickness direction is difficult to be applied in real structures and according to the method used by the designer, there is no efficient estimation of residual stresses distribution. The challenge is estimating the RS distribution in welds in thickness direction knowing only the magnitude of surface RS.

Studying and analyzing the collected data from literature [15–36] welding RS are categorized according to the sign and the magnitude of surface RS. It has been observed that the magnitude of residual stresses dependent on the welding process (welding order, the welding parameters) and the stiffness of the structures (material of the structure). The uncertainty of the welding process leads to uncertainty of the magnitude of surface RS, and the depth and the maximum magnitude of sub-surface RS. This uncertainty in the weld (parameters and weld order) is controlled by a specific probability law distribution. Hence, independent of the welding parameters a mean shape of welding residual stresses could be defined.

Analyzing the reviewed collected data, it was found that for a specific case of RS distribution (i.e. compressive or tensile at the surface) two shapes can be defined. The first shape (distribution) of residual stresses is mastered by the stress at two critical points, point A (at the surface) and point B (at the sub-surface) which have opposite signs. The second shape is defined by three critical points one at the surface (point A) and two sub-surface points A′ and B. The collected data suggest that the stress at the point A′ has always the same sign as that at A, while the RS at point B it has an opposite sign (see Table 1). Shape 1 can be defined with two zones while shape 2 is defined by three zones. Table 1 shows the two shapes with a relation between the magnitude of surface RS and the maximum magnitude of sub-surface RS based on the analysis of the collected data. The zones of each shape are also shown.

It has been observed that the magnitude of welding residual stresses depends on the material of the welded plates. In this paper, a selection of the elastic limit of material (f_y) to study the magnitude of residual stresses is made. The magnitude of residual is normalized by the elastic limit of the material f_y.

It should be noted that the constants $\alpha = \frac{RS_A}{f_y}$, $\beta = \frac{RS_B}{f_y}$, and $\gamma = \frac{RS_{A'}}{f_y}$, can be higher than 1 where the magnitude of residual stresses exceeds the elastic limit of the material which is the case in [17]. With this definition of these three constants and without putting any

Table 1
Shapes of welding residual stresses distribution along the thickness direction at the weld toe.

Shapes of RS distribution at the weld toe through the thickness	Shape1	Shape 2
	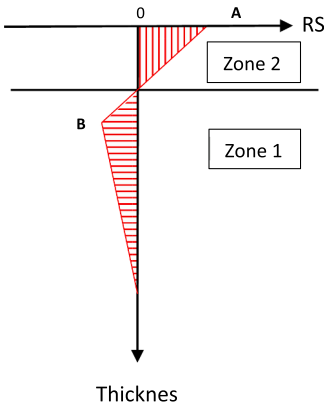	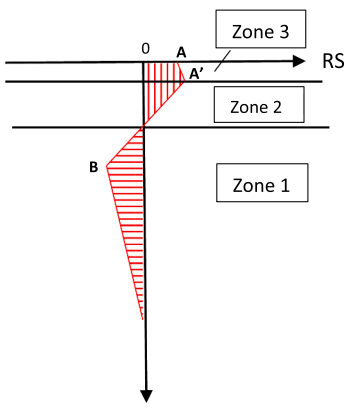
reference points	A and B	A, A′ and B
RS magnitude at A (compressive or tensile cases)	$RS_A = \alpha f_y$ with α is a constant parameter	$RS_A = \alpha f_y$ with α is a constant parameter
RS magnitude at B (compressive or tensile cases)	$RS_B = \beta * f_y$ with β is constant parameter	$RS_B = \beta * f_y$ with β is constant parameter
RS magnitude at A′ (compressive or tensile cases)	x	$RS_{A'} = \gamma * f_y$ with γ is constant parameter

RS_A: The magnitude of residual stresses at the surface, (point A).
$RS_{A'}$: The magnitude of residual stresses at the sub-surface with the same sign as point A, (point A′).
RS_B: The magnitude residual stresses at the sub-surface, (point B).
f_y: The Yield strength of the material.
α: constant $\frac{RS_A}{f_y}$.
β: constant $\frac{RS_B}{f_y}$.
γ: constant $\frac{RS_{A'}}{f_y}$.
x: No value.

Table 2
RS distribution through the thickness; case of tensile RS at the surface.

Data	RS_A [MPa]	$RS_{A'}$ [MPa]	RS_B [MPa]	$D_{A'}$ [mm]	D_B [mm]	Plate thickness [mm]	Material	f_y [MPa]	σ_u [MPa]	Residual stresses state	Weld detail type	Shape	reference
M1	280	310	−150	1	11	20	S700	700	750–900	Transversal	Longitudinal	2	[15]
M2	100	170	−70	0,01	0,6	5	s960	960	1050	x	K joint	2	[16]
M3	80	562	20	0,01	0,2	12,7	DH36	375	510	x	Transverse	2	[17]
M4	25	160	−50	1	40	50	stainless steel	300	X	x	butt weld	2	[18]
M5	548	590	−100	2,5	2,5	20	S690	750	847	x	Butt weld	2	[19]
M6	325	600	−180	1,5	22	33	E309L steel	353	647	longitudinal	Butt weld	2	[20]
M7	280	320	−100	1,4	5	20	S700	700	750	Transversal	T joint	2	[15]
M8	100	180	−20	0,1	1	12	s960	960	X	Transversal	T joint	2	[21]
M9	100	x	−70	x	0,2	10	SU316	307	628	x	Butt weld	1	[22]
M10	479	x	−150	x	4	8	S700	690	x	Transversal	Longitudinal	1	[23]
M11	185	x	−90	x	4	8	S788	690	x	Longitudinal	longitudinal	1	[24]
M12	300	x	−300	x	11	16	SM570	555	626	Longitudinal	Longitudinal	1	[24]
M13	220	x	−120	x	8	16	JIS-SM490A	325	500–600	Longitudinal	Transverse	1	[25]
M14	550	x	−500	x	8	15	SS142171-91	560	700	Transversal	Butt weld	1	[26]
M15	220	x	−150	x	6	16		355	x	x	K joint	1	[27]
M16	280	x	−400	x	0,3	12	S460M	460	x	x	T joint	1	[28]
M17	80	x	−50	x	7	25	S460M	350	x	x	T butt	1	[28]
M18	225	x	−150	x	6	20	45Mn17steel	390	400	x	Cruciform	1	[29]

M1-M18: Data 1 to data 18.
$D_{A'}$: The depth of the $RS_{A'}$ [mm].
D_B: The depth of the RS_B [mm].
σ_u: The ultimate strength [MPa].
x: No value.

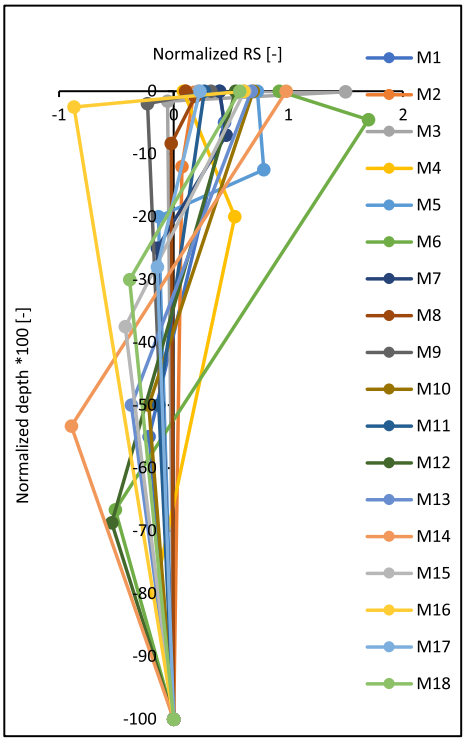

a) Both shapes

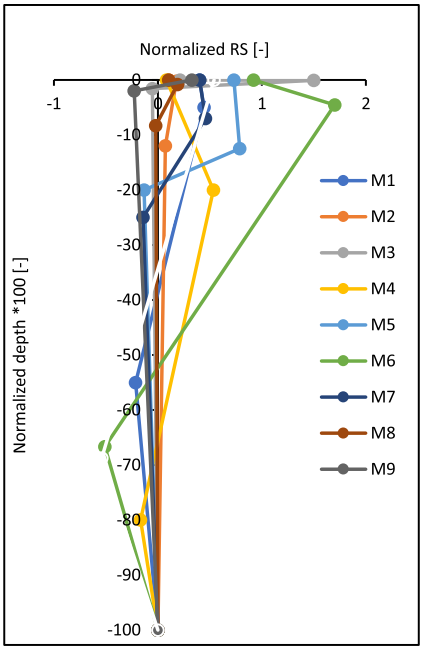

b) Shape 1

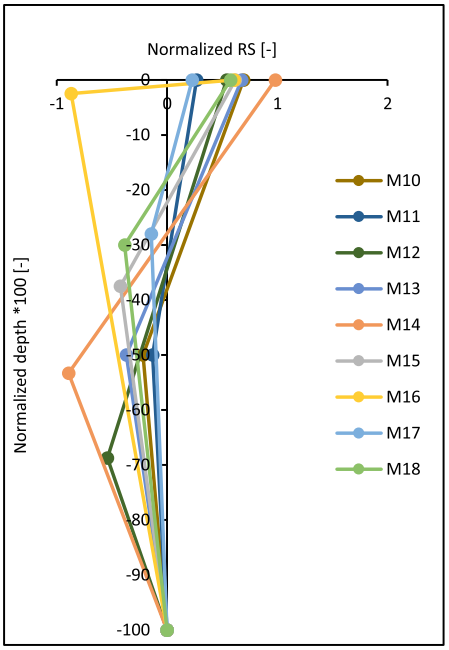

c) Shape 2

Fig. 3. RS distribution along the normalized thickness at the weld toe in the case of tensile RS at the surface, (a) both shapes, (b) shape 1 and (c) shape 2.

condition on them (if they exceed 1 or no), the method is valid even in the case where the magnitude of residual stresses exceeds the elastic limit of the material.

Ultimate stress (σ_u) could be also used to normalize the magnitude of residual stresses which will generate other values of the constants $\alpha = \frac{RS_A}{\sigma_u}$, $\beta = \frac{RS_B}{\sigma_u}$, and $\gamma = \frac{RS_{A'}}{\sigma_u}$. The developed method still applicable with an update of the values of α, β and γ.

3.1. Tensile welding residual stresses at the surface

The analysis of the collected data shows that in most cases welding introduces tensile RS at the surface. Most of them are limited to measure the surface residual stresses to show it is tensile without giving any indication of the shape through the thickness direction. Only 18 of the collected data sets showed the measured RS through the plate thickness in the case of tensile residual stresses at the surface.

Table 2 presents the distribution of RS along the depth at the weld toe for different plate thicknesses, materials, and welded joints. To determine RS shapes independent of these parameters, a normalized RS $\left(\frac{RS_{A,A',B}}{f_y}\right)$ and a normalized depth $\left(\frac{D_{A',B}}{\text{plate thikness}}\right)$ are used to plot the RS distribution for all collected data (see Fig. 3).

A probabilistic analysis of the collected data was performed, and the results are summarized presented in Table 3. Analyzing the collected data in Table 2, regardless of the welding parameters, the following interpretations can be made:

- In the case of tensile RS at the surface, the two shapes of RS distribution presented in Table 1 are found with almost equal probability (shape 1 with probability $= \frac{9}{18} = 0.5$and shape 2 with probability $= \frac{9}{18} = 0.5$).
- Independent of the shape of stress distribution (1 or 2) a linear regression line connecting the value of surface RS (RS_A) and the maximum value of the sub-surface RS (RS_B) is investigated in Fig. 4. This linear relation is found regardless of material properties, thickness and type of weld details. Again, for any of these shapes (1 or 2) the mean of the depth of the point B, D_B, is 35% of the plate thickness with a standard deviation of 27% (see Table 3).
- Regarding shape 2, the intermediary point A′ has almost the same mean magnitude of RS as point A (which can be translated to $\frac{RS_A}{RS_{A'}} \cong 1$) (see table 3 mean of $RS_A = 0.35$ and mean of $RS_{A'} = 0.39$) and is found at around 2.2% of the normalized thickness. Hence, zone 3 (see Table 1) has a rectangular shape, see Fig. 5, with very shallow depth compared to the plate thickness.
- Knowing the magnitude of RS at the surface doesn't give any indication concerning the shape either 1 or 2 especially that the probability of occurrence for shape 1 and shape 2 are almost equal. In line with the study in and Table 1, especially for the shape 2 that zone 3 is very shallow (around 2.2% of the normalized depth) leads to simplifying shape 2 to shape 1 by neglecting the point A′ in the estimated RS shape, see Fig. 6 green shaded area. Hence, Shape 1 is a good approximation for all cases.

Adapting the simplifications mentioned and discussed above (i.e. a linear relationship between RS_A and RS_B and the use of Shape 1 (Fig. 7) as a valid representation for all residual stresses distributions), the value and distribution of residual stresses can be obtained with any specific (or requested) reliability. Fig. 7, "R^{2}" is the square of the linear regression factor.

3.2. Compressive welding residual stresses at the surface

It has been a common view that welding introduces high tensile residual stresses on the surface at weld toes. Analysis of the collected data shows however that a relatively large number of measurements revealed compressive residual stresses at the surface. Table 4 summarizes the parameters describing the shape of residual stresses distribution for the cases with compressive surface stresses. In the study of the published data, it was found that welding rarely introduces a compressive RS at the surface compared to the case of the surface tensile RS. Fig. 8 summarizes the shapes of welding RS in the case of compressive RS at the surface.

Analyzing the collected data in Table 4 and Fig. 8 (regardless of the welding parameters), the following observations can be made:

- Irrespective of the shape (1 or 2), $\frac{RS_B}{f_y}$ has a mean value of 0.59 and a standard deviation of 0.39. Concerning the location of this point, it has a mean value of 10% of the normalized thickness varying with a standard deviation of 7%, see Table5.

Table 3
Probability density function of the random variables defining the RS shape.

Random variable	Probability law	Mean	Standard deviation σ
$\frac{RS_A}{f_y}$	Lognormal	0.35	0.27
$\frac{RS_{A'}}{f_y}$	Lognoraml	0.39	0.47
$\left\lvert\frac{RS_B}{f_y}\right\rvert$	Lognormal	0.2	0.25
$\frac{D_B}{\text{plate thickness}}*100$	Normal	35	24
$\frac{D_{A'}}{\text{plate thickness}}*100$	Normal	2.2	6.5

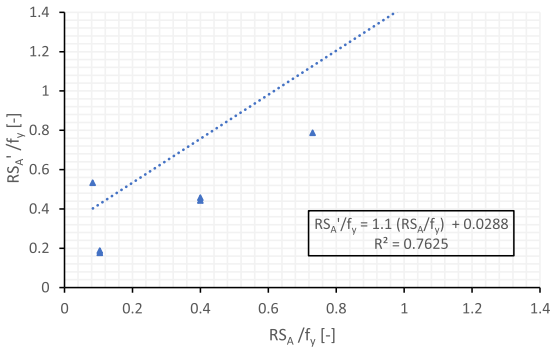

Fig. 4. Value of RS at the surface (RS_A) as a function of the value of residual stresses at A′ ($RS_{A'}$).

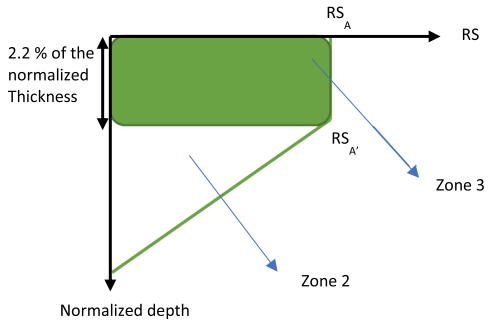

Fig. 5. Schematic representation of zone 3 in case of tensile RS at the surface, shape 2.

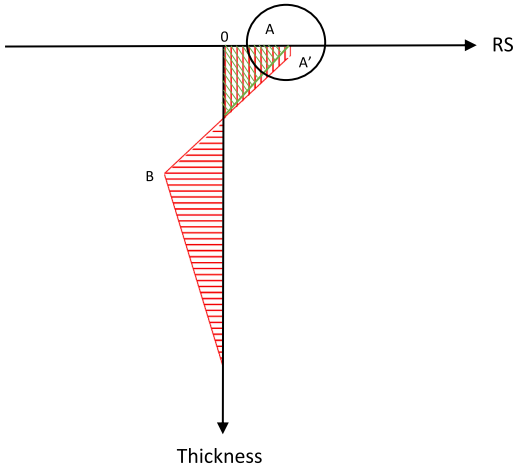

Fig. 6. Simplification of the shape 2 to shape 1 in the case of tensile RS at the surface.

- When the distribution of residual stresses follow shape 1, equilibrium is defined by points A and B. $\frac{RS_A}{f_y}$ has a mean value of 0.57 independent of the plate thickness, material proprieties and welded detail.
- When the distribution of residual stresses follows shape 2, three critical points are identified. $\frac{RS_A}{f_y}$ has a mean value of 0.18 and a standard deviation of 0.19. While $\frac{RS_{A'}}{f_y}$ has a mean value of 0.57 found at 0.3% of the normalized depth with a standard deviation of 0.4%. $\frac{RS_A}{RS_{A'}}$ is almost constant and equal to 0.3 which leads to a linear relation between RS_A and $RS_{A'}$. Hence, zone 3 has a shallow width compared to the plate thickness and lower magnitude of surface residual stresses which leads to a small area of zone 3 compared to zone 1 and 2. See Fig. 9.
- Irrespective of the shape (1 or 2), a linear relation connecting max (RS_A, $RS_{A'}$) and RS_B has been found in Fig. 10.
- $RS_{A'}$ in case of shape 2 has the same value as RS_A in the case of shape 1, which mean in the case of shape 2, zone 3 is too little in term of the area compared to zone 1 and 2 (see Table 1). This leads to simplifying shape 2 to shape 1 (see the shaded area in Fig. 11). This leads to the shape of the RS being described by the maximum of RS_A and $RS_{A'}$ together with RS_B in the case of

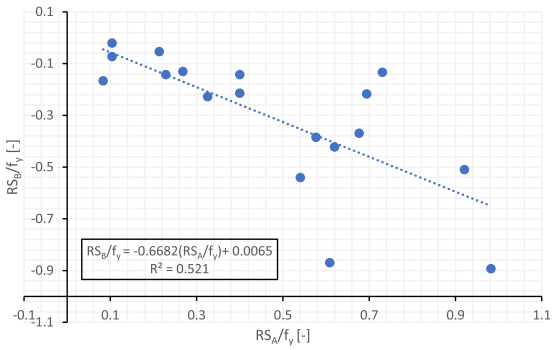

Fig. 7. Value of RS at the surface RS_A (tensile) as a function of the maximum value of sub-surface residual stresses RS_B (compressive).

compressive surface RS.

Using the collected experimental data, lognormal distribution laws for the value of surface RS and the maximum value sub-surface RS and normal law distribution for the depth of sub-surface RS are constructed. Table 5 summarizes the probability density functions for these random variables.

3.3. The effect of the residual stresses in the damage distribution and crack initiation

The residual stresses are permanently present in structures, which leads to affecting the mean stress without changing in the stress amplitude. For structures have residual stresses and submitted to external cyclic loading ($\sigma_{a,ext}$, $\sigma_{m,ext}$), two cases could be presented. The first case, if the local residual stresses are positive (tensile), it increases the mean stress σ_m which is an unfavorable situation for fatigue. The second case, if the local residual stresses are negative it leads to a reduction in the mean stress σ_m which is a favorable situation for fatigue.

Residual stresses in welded joints can be relatively high. On the first hand, if local residual stresses are compressive, the applied stress range after mean stress correction is very low. In this case, micro-cracks can hardly grow. As the residual stresses do not affect the stress range, cyclic slip in the material can however still occur. On the other hand, if local residual stresses are tensile, the stress range after mean stress correction is very high which leads to accelerated crack initiation and propagation. Hence, in general, there is a high probability that fatigue damage will occur first at points where there is high tensile RS.

The residual stresses can be beneficial or harmful as long as they are stable. However, the relaxation of such stresses due to mechanical loading is a well-known phenomenon recognized under cyclic loading [38–42]. It has been shown that the main relaxation of the residual stresses normally takes place in the first cycle, followed by a further gradual relaxation during fatigue life [39–40]. However, this is not a universal rule and depends on many factors: the initial residual stresses, the actual material, and microstructure (damage), as well as the loading condition. It has been found that the amount of residual stresses relaxation is very low when the applied load cycles do not cause macro-plasticity [40–42] while the higher amount of residual stresses relaxation noted with high-stress ranges (causes macro-plasticity). It is very important to include residual stresses relaxation phenomena for an accurate estimation of fatigue life. However, it is very challenging to combine welding residual stresses relaxation with the developed probabilistic model. For this reason, in this paper, the residual stresses relaxation was not taking into account until the crack initiation phase. This assumption predicts more accurate fatigue life compared to the case where no residual stresses are considered but it underestimates the fatigue life compared to the situation where residual stresses relaxation are considered.

For a given welded detail, linear-elastic finite element simulation can be used to determine the stress concentration factor k_t and the effective notch stress to derive the stress notch factor k_f. By knowing the external stress range and mean stress ($\sigma_{a,ext}$, $\sigma_{m,ext}$), σ_{RS}, k_t and k_f and using Morrow law for the mean stress correction an equivalent, fully reversed stress amplitude with zero mean stress can be determined.

For example in the case of shape 1 (see Table 1), the determination of the point where the damage reaches 1 first requires computing the number of cycles to failure at the two critical points (N_A;N_B) using the S-N curve of the material and the stress amplitudes σ_a(where the residual stresses are introduced in the mean stress correction). The point which has a minimum value of the number of cycles (min (N_A; N_B)) presents the critical point where the damage reaches 1 first (for example point A). At this number of cycle (N_A) the damage at the other point (B) is equal to:

$$D_B = \frac{N_A}{N_B} \tag{5}$$

where D_B is damage at point B when the damage at point A reaches 1, N_A is the number of cycles to introduce damage = 1 at A and N_B is the number of cycles to introduce damage = 1 at

Table 4
RS distribution along the thickness direction in the case of the compressive RS at the surface.

	RS_A [MPa]	$RS_{A'}$ [MPa]	RS_B [MPa]	$D_{A'}$ [mm]	D_B [mm]	Plate thickness [mm]	Material	f_y [MPa]	σ_u [MPa]	Residual stresses s tate	Detail Type	Shape	Reference
M1	−25	−250	250	0,06	0,8	5	S355	355	575	Transversal	Longitudinal	2	[30]
M2	−50	−490	200	0,01	0,6	5	S960	960	1050	Transversal	Longitudinal	2	[31]
M3	−150	−150	50	0,05	1	12,4	S355	355	575	Longitudinal	Longitudinal	2	[33]
M4	−130	X	450	x	9,5	24	—	449	525	Axial	strip of pipe	1	[36]
M5	−120	X	480	x	10,5	24	—	449	525		strip of pipe	1	[34]
M6	−295	X	205	x	8	100	A508 Cl.3 low alloy steel	536		x	Butt weld	1	[35]
M7	−220	X	510	x	10	24	——	449	—	Axial	Strip of pipe	1	[36]
M8	−50	X	590	x	8	24	———	449	—	Axial	Stripeof pipe	1	[36]
M9	−130	X	410	x	12	24	——	449	—	Axial	Strip of pipe	1	[36]

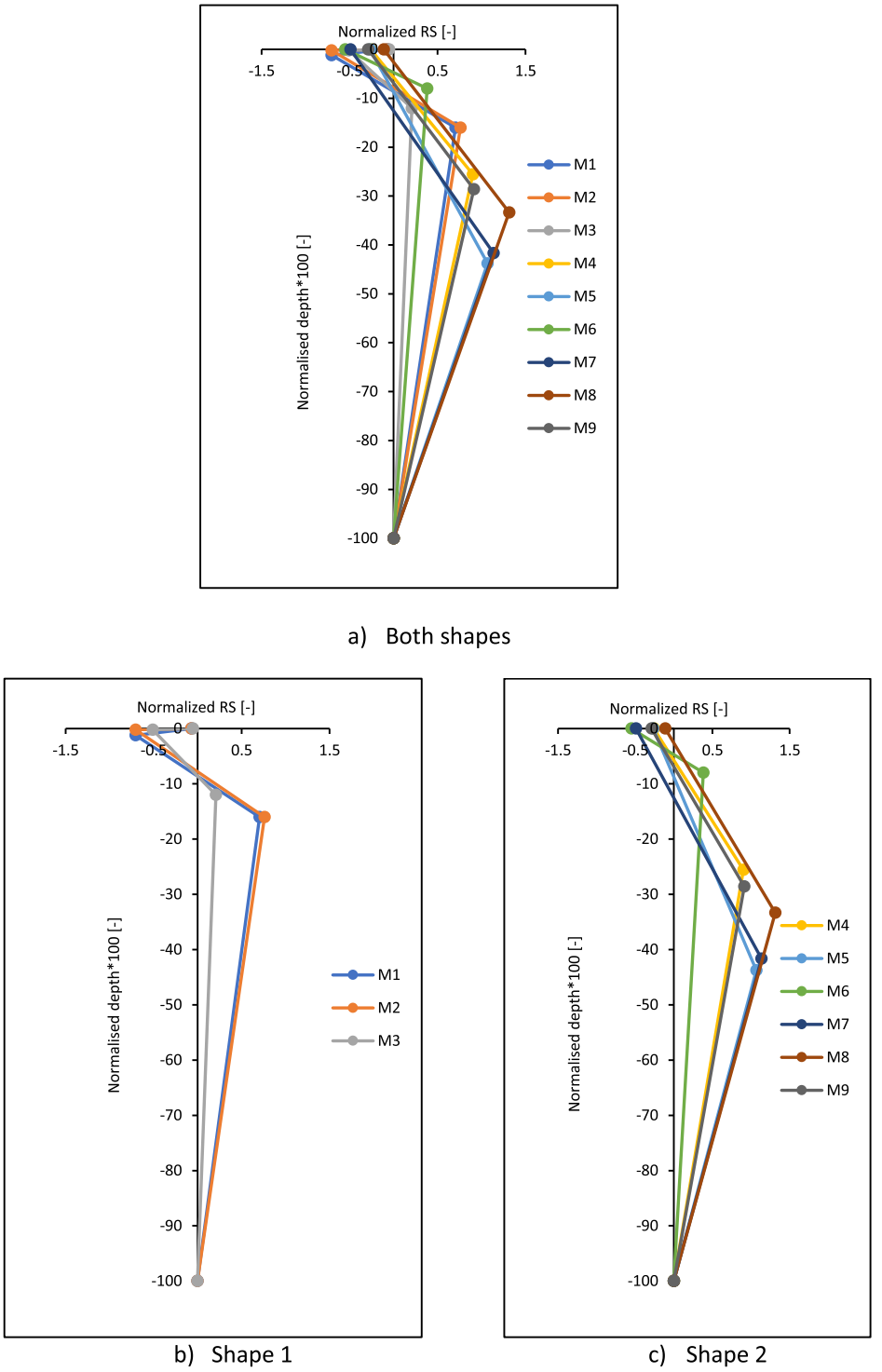

Fig. 8. RS distribution through-thickness direction in the case of compressive RS at the surface: (a) both shapes 1 and 2, (b) shape 1 and (c) shape 2.

Table 5
Probability density function of the random variables defining the RS distribution for cases with compressive residual stresses at the surface.

Random variable	Probability law	Mean	Standard deviation
$\left\|\frac{RS_A}{f_y}\right\|$	Lognormal	0.18	0.19
$\left\|\frac{RS_{A'}}{f_y}\right\|$	Lognormal	0.57	0.12
$\frac{RS_B}{f_y}$	Lognormal	0.59	0.39
$\frac{D_B}{\text{plate thickness}}*100$	Normal	10	7
$\frac{D_{A'}}{\text{plate thickness}}*100$	Normal	0.3	0.4

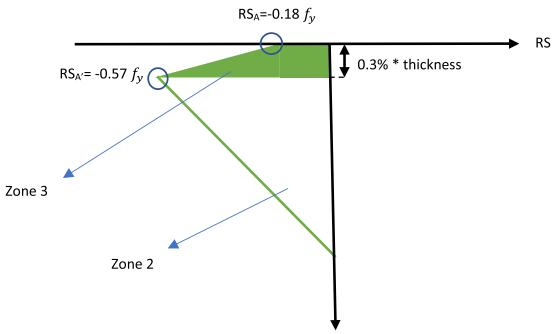

Fig. 9. Schematic representation of zone 3 in case of compressive RS at the surface, shape 2.

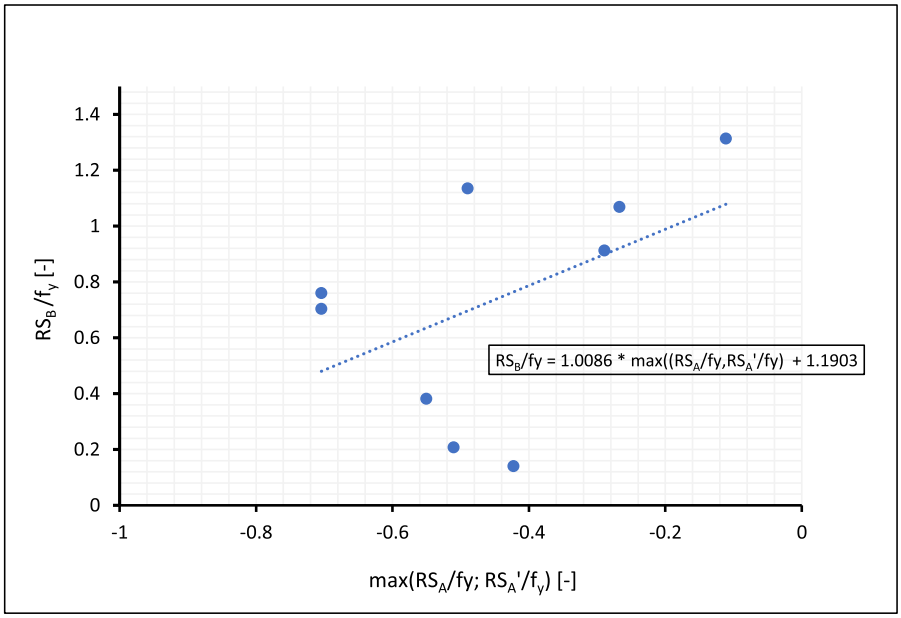

Fig. 10. Correlation between RS_A and RS_B in the case of surface compressive RS.

4. Experimental investigation of the proposed method

Within the project "LifeExt", an extension of fatigue life of existing welded prefatigued structures has been studied. The specimens in this project consist of a transversal attachment of the fillet weld joint with the dimension showed in Fig. 12. These tests (as welded) that have been recently conducted showed a high fatigue strength and high slope of the S-N curve compared to the fatigue strength and the slope of the S-N curve of the standard as-welded structures [37].

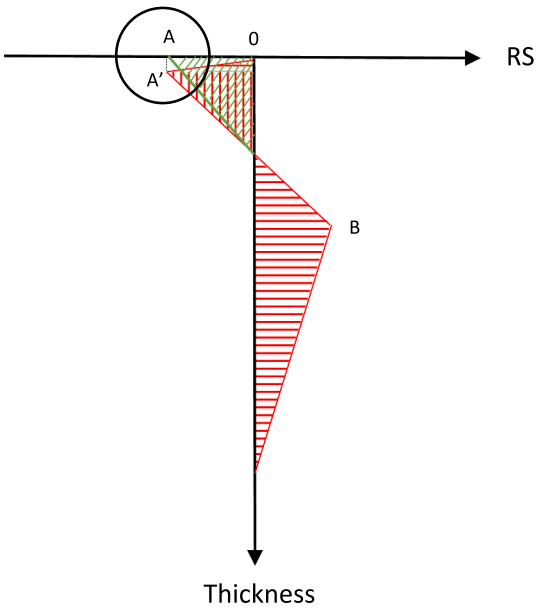

Fig. 11. The simplification of the shape 2 to shape 1 in the case of compressive residual stresses at the surface.

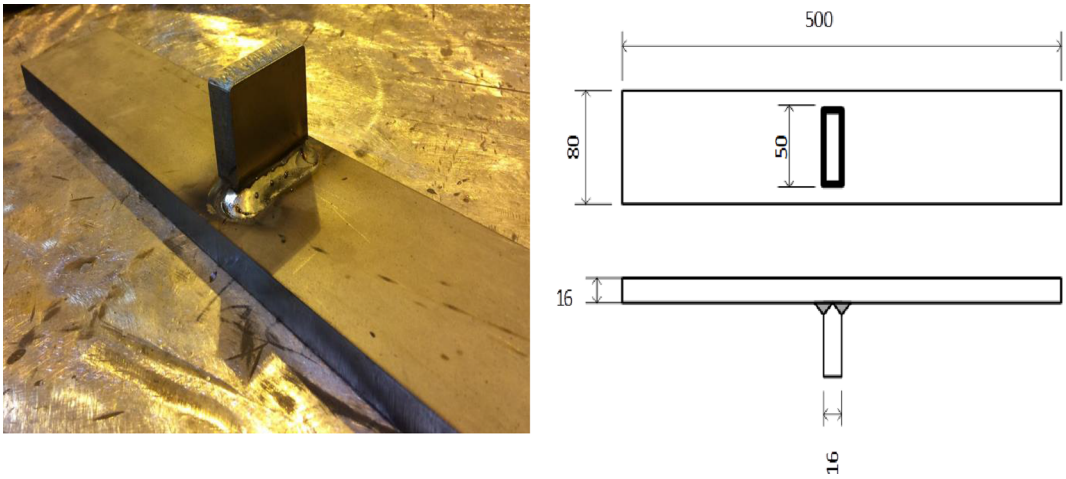

Fig. 12. Dimensions of the studied specimen [mm].

Table 6
A statistical study of the geometrical parameter for the specimens in the as-welded state.

	Toe radius [mm]	Undercuts [mm]	Throat thickness [mm]	Weld angle [degree]	Stress concatenation [–]
Mean	0.67	0.0035	4.86	67	1.27
Standards deviation	0.31	0.0306	0.401	1.8	0.26

4.1. Test specimens and testing procedure

The test specimens selected to be studied in this paper consist of a load-carrying plate with a transversal attachment with a steel-based plate (S355). The plate geometry is shown in Fig. 12. The specimens are tested to tensile fatigue tests with stress ratio R = 0.29. See specimens are tested in a resonance pulsator at a testing frequency of approximately 31 Hz and they have been instrumented with one strain gauge (on each side).

The statistic study of the weld geometry presented in Table 6 is determined using a 3D laser geometry scanner. Fig. 13 shows a schematic representation of these parameters.

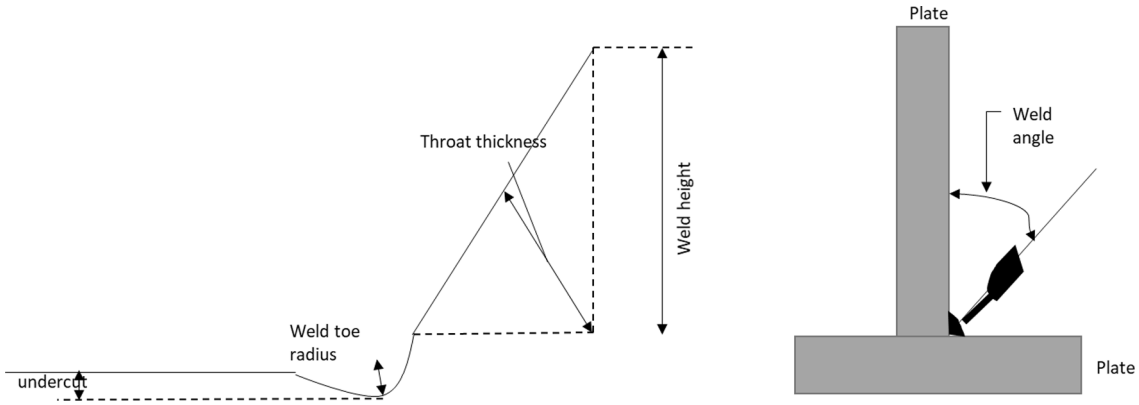

Fig. 13. Geometrical investigated parameters in laser weld scanning.

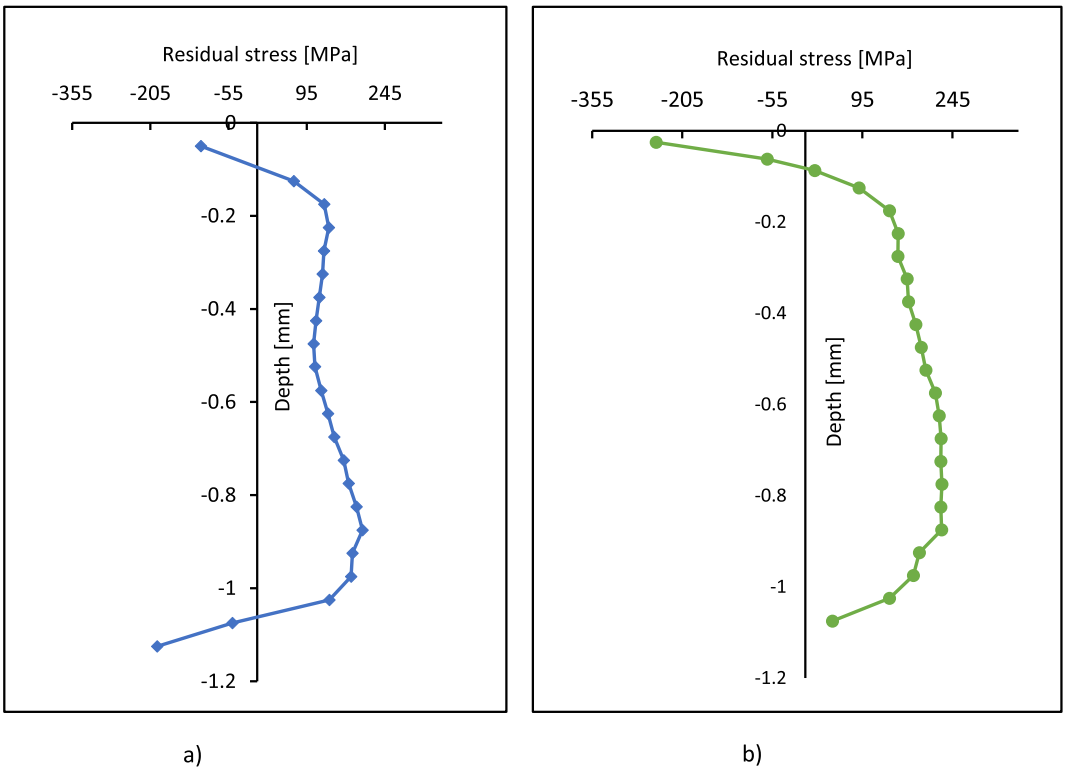

Fig. 14. Measured residual stresses through thickness direction at the weld toe in two different specimens (a) 250 MPa compression at the surface, (b) 100 MPa compression at the surface.

Table 7
Welding parameters.

Run	Diameter of the electrode [mm]	Weld current [A]	Welding voltage [V]	Welding speed [mm/sec]	Wire feed speed [mm/min]	Heat input [KJ/mm]
1	1.2	240	28.3	140	9.2	0.9
2	1.2	230–240	28.3	130–140	9.2	0.9–1

4.2. Measurements and estimation of residual stresses shapes

Measurement of the welding residual stresses on two randomly selected specimens using X-ray diffraction (to measure the RS at the surface) and hole drilling technique (to measure RS at the surface and through the thickness direction down 2 mm and at 1 mm

from the weld toe) has been investigated and showed in Fig. 14. The welding parameters are listed in Table 7. Both specimens showed compressive surface RS at the weld toe with a magnitude of −250 MPa for the first selected specimen and −100 MPa for the second selected specimen.

The probabilistic study developed in Section 3 is verified with these experimental fatigue test data which show the case of compressive residual stresses at the surface.

In agreement with the probabilistic study described in Section 3, an RS shape has been constructed knowing only the magnitude of RS at the surface. According to the relationship that has been extracted in Fig. 10 connecting RS_A and RS_B, a prediction of the magnitude RS at B can be estimated to 254 MPa at a depth of 0.85 mm (correspond to 50% of probability of occurrence) for the specimen with 250MPA compression at the surface. A measurement of RS through-thickness direction for the same specimen (with 250 MPa compression at the surface) corresponds to tensile with the value 227 MPa ($=0.63f_y$) noted in depth of 0.825 mm from the surface (Fig. 14b).

Another RS measurement by hole drilling for another specimen with 100 MPa compressive at the surface corresponds to 202 MPa ($=0.56\ f_y$) tensile at 0.875 mm depth (Fig. 14a) while the estimation shape at this specimen is presented in Table 8.

This wide difference between the estimated and the measured shape of the residual stresses could be explained by the reason that the estimated value is based on a probabilistic study were the standard deviation is important (see Table 5) which reflects the dispersion of the data which might be causative for errors.

4.3. Measurement and estimation of crack initiation and fatigue life in the presence of compressive residual stresses at the surface

The measured shape of the residual stresses distribution affects fatigue life which is presented in the experimental found fatigue life. To study the effect of the estimated shape on fatigue life, a use of the estimated residual stresses shape with a cumulative fatigue damage model and fracture mechanics presented in Section 3.3 has been conducted to plot the estimated fatigue life and then S-N curve. According to Section 3.3, that crack initiation is expected to be sub-surface, i.e. at point B.

This could be verified experimentally by studying the evolution of local strains close to the weld toe in specimens, which is obtained and reported in the curve in Fig. 16 connecting the number of cycles as a function of the average strain drop for the first specimen. To study the crack location of crack initiation with strain drop the certain number of specimens have been instrumented with strain gauges (five to seven on each side) with a lateral spacing of 1 cm along the weld and a distance of 3 mm from the weld toe to the middle of the gauge (Fig. 15). When crack initiates below the surface, the surface stresses registered by the strain gauge closest to the crack will first increase followed by a sharp drop in strain, when the crack propagates to reach the surface (Fig. 16a). When crack initiates at the surface, a drop in the strain gauge closest to the point of crack initiation is expected (and registered) due to crack initiation and propagation through the thickness (Fig. 16b). More detail on the method could be found in [43].

In Fig. 17, the damage distribution along the thickness direction is computed for three cases for the specimen with −250 MPa residual stresses at the surface. The curves correspond to the damage distribution along the thickness direction for the case of the estimated shape of welding residual stresses under cyclic loading with stress range 150 MPa and mean stress 55 MPa. The first curve with triangle points leads to the conclusion that the crack initiation (Damage = 1) is reached first at the sub-surface. This is verified by the strain measurement that has been measured close to the weld toe (see Fig. 16a) which showed strain increase represents the outcome of sub-surface cracks in some location at the weld toe.

The second curve represented as well the damage distribution through the thickness under the same loading level as the first test but at this test, the residual stresses at the point B are estimated to 5% probability of occurrence according to the law determined in Section 3, which showed that the damage reached 1 first at the surface through the orange curve with 'x' points. While the third curve (blue curve with square points) represents the damage distribution for the same case (250 MPa compression at the surface) with estimated residual stresses at the point B to 95% probability of occurrence based in the probabilistic analysis in Section 3. In this case, conducted to introduce sub-surface crack (damage reached 1 first at the sub-surface point B).

For these three cases (which are different only in the value of the sub-surface welding residual stresses) a plot of the S-N curve including the welding residual stresses in the calculation of fatigue life is presented in Fig. 18. The black diamond-points represents the experimental results. The blue upper curve with the triangle points represents the estimated S-N curve which corresponds to (250 MPa compression of RS at the surface, 95% RS sub-surface, 50% of depth). The red lower curve with 'x' points represents the estimated S-N curve which corresponds to (250 MPa compression of RS at the surface, 5% RS sub-surface, 50% of depth). The yellow mean curve with circle points represents the estimated S-N curve which corresponds to (250 MPa compression of RS at the surface, 50% RS sub-surface at 50% depth).

Hence, the fatigue life in the case of compressive residual stresses at the surface for steel S355 for this transversal attachment

Table 8
Comparison between the measured and the estimated shape of RS.

Characteristic of the shape	First test (250 MPa in compression at the surface)			Second test (100 MPa in compression at the surface)		
	Estimated values	Experiment measurement	Error %	Estimated measurement	Experiment measurement	Error %
RS_A [MPa]	−250	−250	–	−100	−100	
RS_B [MPa]	254	227	10	50	202	75
D_B [mm]	0.85	0.825	3	0.85	0.875	3

Fig. 15. Position of the strain gauges to detect crack initiation.

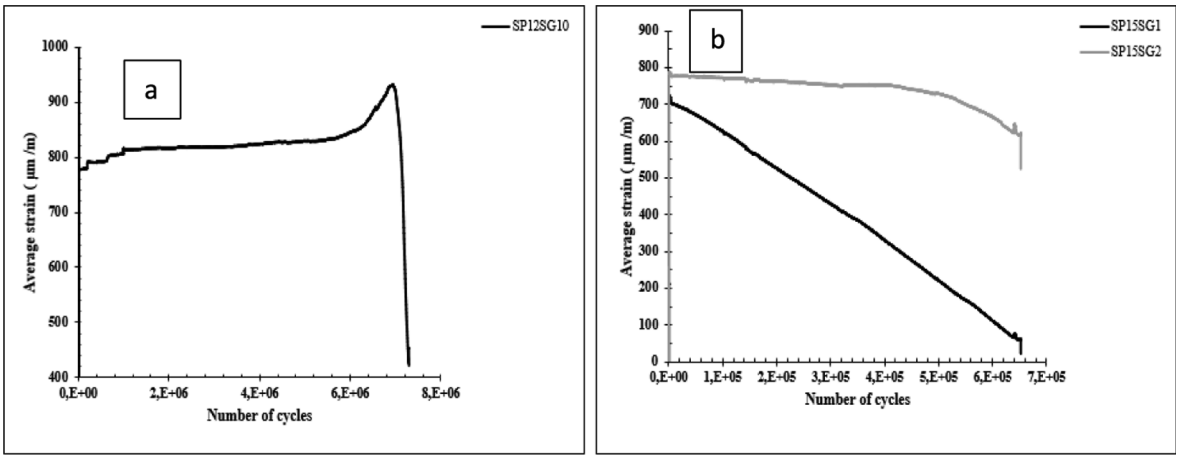

Fig. 16. The local strain evolution at the weld toe during the test, (a) case of initial sub-surface, (b) case of initial surface crack.

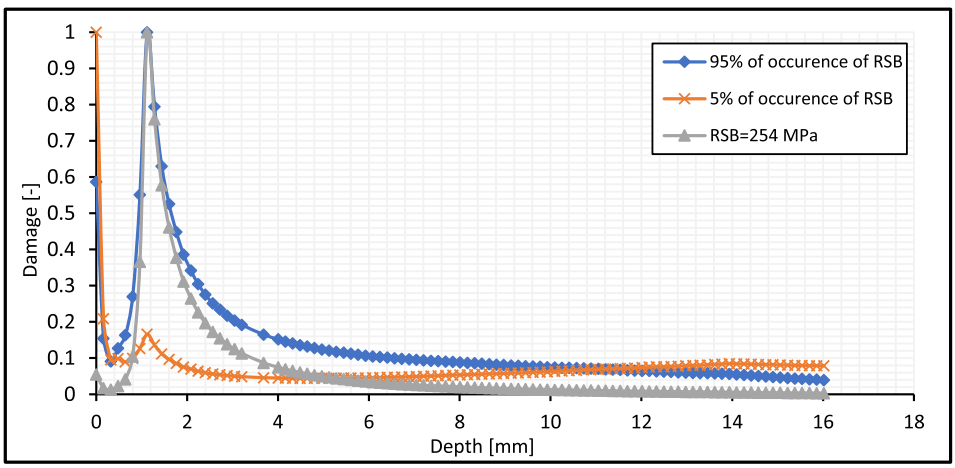

Fig. 17. Damage distribution along the depth for the save and the non-save case.

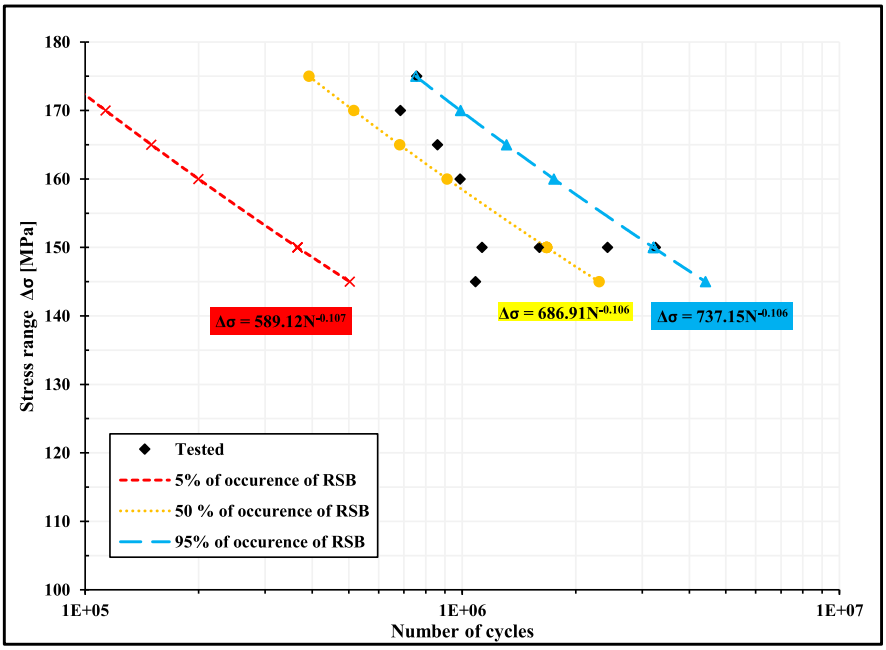

Fig. 18. Experimental and estimated fatigue life versus the stress ranges for 5%, 50% and 95% of probability of occurrence of RS_B for the case of 250 MPa compression at the surface.

(Fig. 12) is between these two bounds (the upper and the lower estimated S-N curve, see Fig. 18). The scatter of the experimental data is likely to be related to the parameters of the welding process or the material itself. This manifests also in the measured residual stresses, RS, where two specimens showed a difference of 60% in the measured residual stresses (250 MPa and 100 MPa compression).

As the standard deviation is high due to dispersion of the collected data and to lack of data, the estimated value to define residual stresses shape can be updated by the two measured residual stresses shapes that have been presented in Fig. 14.

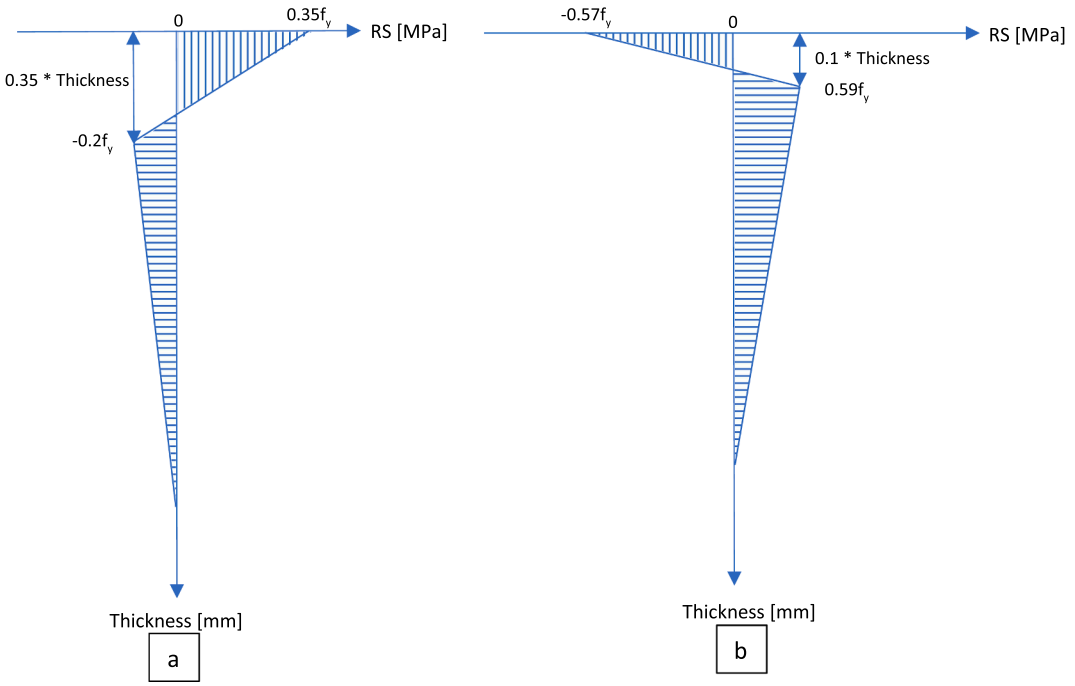

Fig. 19. The estimated mean shapes of welding residual stresses at the weld toe through the thickness direction (a) case of tensile residual stresses at the surface, (b) case of compressive residual stresses at the surface.

5. Summary and conclusion

In the design phase, it is assumed that welding RS is in the order of magnitude of the material yield strength regardless of welding parameters. Also, it is assumed that these stresses are tensile in the critical locations (weld toe, for example). The method used in engineering is an empirical method overestimating the residual stresses distribution affecting the designed fatigue life of structures. **Therefore, in this paper, a probabilistic study of welding residual stresses regardless of the welding parameters was carried out**. The collected measured data from the literature of welding residual stresses distribution along the thickness direction at the weld toe for welded joints has been studied. Further evaluations of these residual stresses, RS data distribution for longitudinal attachments, transverse attachments, butt joints, K joints, and cruciform joints have been performed in order to estimate the shape of welding RS distribution by knowing the surface RS. The yield strength(f_y) of the tested base materials varied from 307 to 1050 MPa and specimen thickness has varied from 5 to 100 mm. Based on this literature study two cases of welding RS can be generalized with the following main findings:

– In the case of tensile welding RS at the surface and regardless of the welding parameters
- The two shapes 1 and 2 presented in Table 1 can occur with equal probability.
- Independent of the shape, the depth of the RS_B has a normal distribution with a mean value of 35% of the normalized depth with an absolute magnitude with a mean value of $0.12f_y$ and a standard deviation of $0.25f_y$.
- In the case of shape 2, the value of the residual stresses at point A and A′ can be equal
- Irrespective of the shape of residual stresses (1 or 2), a linear relation connects the value of $\frac{RS_A}{f_y}$ and the value of $\frac{RS_B}{f_y}$ is assumed (see Fig. 7).
- Regardless of the welding parameters, the estimated mean shape is shown in Fig. 19a.

– In the case of compressive welding RS at the surface and regardless of the welding parameters
- The two shapes 1 and 2 presented in Table 1 can occur with equal probability in analogy to what is found for the case of tensile stress at the surface.
- Independent of the shape, the depth of the RS_B has a normal distribution with a mean value of 10% of the normalized depth and a magnitude with a mean value of $0.59f_y$ and a standard deviation of $0.12f_y$.
- In the case of shape 2, the surface RS_A is $-0.18\ f_y$. The $RS_{A'}$ has an absolute mean reach $0.57\ f_y$.
- The random variable RS_A in the case of shape 1 has the same distribution as $RS_{A'}$ in the case of shape 2
- Irrespective of the shapes, a linear relationship between the surface max ($RS_{A'}$, RS_A) and the sub-surface RS (RS_B) stress can be assumed.
- Regardless of the welding parameters, the estimated mean shape is shown in Fig. 19a for the case of tensile residual stresses is introduced at the surface and Fig. 19b for the case of compressive residual stresses is introduced at the surface.

– Independent of the surface residual stresses whether compressive or tensile
- Based on the evaluation of existing RS measurements from the literature, both tensile and compressive surface stresses can be introduced in welded joints. The probability of occurrence of tensile residual stresses at the surface is $\frac{18}{27}$ while the probability of occurrence of compressive residual stresses at the surface is lower and it reaches $\frac{9}{27}$.
- A simplification of shape 2 to shape 1 can be made (with green shaded area see Figs. 9 and 11).
- By only knowing the surface residual stresses (from X-ray diffraction, e.g.) and based on the developed model, RS distribution through the thickness of a welded joint can be predicted.
- The model has been verified with a measured RS distribution through the thickness in two welded specimens with steel S355.

– In the fatigue life
- With this model, an estimation of the fatigue damage with an upper and lower bound can be made taking into account the value and distribution of RS. Fatigue test results on specimens with measured residual stresses have been used to demonstrate the capabilities of the developed model.
- The fatigue life of welded joints is strongly affected by residual stresses at the weld toe (See Fig. 18).
- The inclusion of residual stresses in fatigue analysis permits a prediction of fatigue life of weldments more accurately (Fig. 18).
- Due to a lack of RS data distribution through the depth in the case of compressive RS at the surface, the estimated probability density function can be changed according to other additional data.

Declaration of Competing Interest

The authors declare that they have no known competing financial interests or personal relationships that could have appeared to influence the work reported in this paper.

Acknowledgment

This work is a part of the research project “LifeExt” which is funded by Vinnova (project 2017-02670) and the Swedish Transport Administration (BBT 2017-018).

The authors would like to thank the Ph.D. student Nils Friedrich from the Hamburg University of Technology for his excellent support of the experimental work.

References

[1] Handbook of Laser Welding Technologies, Woodhead Publishing, Editors Seiji Katayama, 2013, pp. 654.
[2] Weman K. and Linden G., MIG welding guide, Woodhead publishing in materials.
[3] N.S.M. Nasir, M.K.L.A. Razab, S. Mamat, M. Iqbal, review on welding residual stress, ARPN J. Eng. Appl. Sci. 11 (9) (2016).
[4] C. L.Sanger, R. J.McDonald, P. Kurath, Prediction of welding residual stresses and redistribution/relaxation due to cyclic loading. Paper number 2005-01-1322. SAE International, 2004.
[5] P.J. Withers, H.K.D.H. Bhadeshia, Residual stress part1- Measurement techniques, Mater. Sci. Technol. 17 (2001) April.
[6] P.J. Withers, H.K.D.H. Bhadeshia, Residual stress part2- Measurement techniques, Mater. Sci. Technol. 17 (2001) April.
[7] I.C. Noyan, J.B. Cohen, Residual stress measurement by diffraction and interpretation. ISBN 0-387-96378-2. Materials research and engineering. Springer-Verlag.
[8] P.J. Bouchard, The NeT bead-on-plate benchmark for weld residual stress simulation, Int. J. Press. Vessels Pip. 86 (1) (2009) 31–42.
[9] A. Hobbacher, Recommendations for fatigue design of welded joints and components. IIW document IIW-1823-07, December 2008.
[10] Walid El-Ahmer, PhD theses, robustesse de la simulation numérique du soudage TIG de Structures 3D en acier 316L.
[11] M.C. Smith, A.C. Smith, NeT bead-on-plate round robin: Comparison of residual stress predictions and measurements, Int. J. Press. Vessels Pip. 86 (2009) 79–95.
[12] D. Radaj, Review of fatigue strength assessment of nonwelded and welded structures based on local parameters, Int. J. Fatigue 18 (1996) 153–170.
[13] Jaap Schijve, Fatigue of structures and materials, Springer, 2009.
[14] D. Radaj, Welding residual stress and distortion: calculation and measurement, ISBN 3-87155-791-9 DVS-Verlag GmbH, Düsseldrof, 2003, pp. 332–350.
[15] E. Mikkola H. Remes G. Marquis A finite element study on residual stress stability and fatigue damage in high-frequency mechanical impact (HFMI)-treated welded joint Int. J. Fatigue 94 Part 1 2017 16 29.
[16] M. Leitner, S. Gerstbrein, M.J. Ottersböck, M. Stoschka, Fatigue Strength of HFMI-treated High-strength Steel Joints under Constant and Variable Amplitude Block Loading, Procedia Eng. 101 (2015) 251–258.
[17] W. Gao, D. Wang, F. Cheng, C. Deng, Y. Liu, W. Xu, Enhancement of the fatigue strength of underwater wet welds by grinding and ultrasonic impact treatment, J. Mater. Process. Technol. 223 (2015) 305–312.
[18] R.H. Leggatt, Residual stresses in welded structures, Int. J. Press. Vessels Pip. 85 (3) (2008) 144–151.
[19] M. Farajian, Mechanical of RS relaxation and redistribution in weld HSS.
[20] J.L. Curtat, J. Lanteigne, H. Champliaud, Z. Liu, J.B. Lévesque, Influence of hammer peening on fatigue life of E309L steel used for 13%Cr-4%Ni blade runner repairs, Int. J. Fatigue 100 (Part 1) (2017) 68–77.
[21] K. Yuana, Y. Sumib, Simulation of residual stress and fatigue strength of welded joints under the effects of ultrasonic impact treatment (UIT), 92(Part 1) (2016) 321–332.
[22] Suzuki T., Okawa T., Shimanuki H., Effect of Ultrasonic Impact Treatment (UIT) on Fatigue Strength of Welded Joints, August 2014, https://doi.org/10.4028/www.scientific.net/AMR.996.736.
[23] R. Fueki, K. Takahashi, Prediction of fatigue limit improvement in needle peened welded joints containing crack-like defects, Int. J. Struct. Integrity 9 (1) (2017) 50–64.
[24] Yıldırım H. Can, G. Marquis, A round robin study of high-frequency mechanical impact (HFMI)-treated welded joints subjected to variable amplitude loading, Weld World (2013), https://doi.org/10.1007/s40194-013-0045-3.
[25] K. Anami, C. Miki, H. Tani, H. Yamamoto, Improving fatigue strength of welded joints by hammer peening and TIG dressing, Struct. Eng./Earthquake Eng. 17 (2000).
[26] K.L. Yuan, Y. Sumi, Modelling of ultrasonic impact treatment (UIT) of welded joints and its effect on fatigue strength, in: The 5th International Conference on Crack Paths (CP 2015), 16-18 September 2015, Ferrara, Italy.
[27] Z. Barsoum, Residual stress prediction and relaxation in welded tubular joint, Weld in the World 51 (1–2) (2007), https://doi.org/10.1007/BF03266545.
[28] H. Günther, U. Kuhlmann, A. Dürr, Rehabilitation of Welded Joints by Ultrasonic Impact Treatment (UIT) IABSE SYMPOSIUM LISBON, 2005.
[29] A.K. Hellier, B.G. Prusty, G.M. Pearce, M. Reid, A.M. Paradowska, P. Simons, Effect of Ultrasonic Peening on Residual Stresses at a T-Butt Weld Toe, Mater. Res. Proc. 2 (2016) 19–24.
[30] M. Leitner, Z. Barsoum, F. Schäfers, Crack propagation analysis and rehabilitation by HFMI of pre-fatigued welded structures, Welding in the World 60 (3) (2016) 581–592.
[31] M. Leitner, M. Khurshid, Z. Barsoum, Stability of high frequency mechanical impact (HFMI) post-treatment induced residual stress states under cyclic loading of welded steel joints, Eng. Struct. 143 (15) (2017) 589–602.
[32] S.H. Han, J.W. Han, Y.Y. Nam, I.H. Cho, Fatigue life improvement for cruciform welded joint by mechanical surface treatment using hammer peening and ultrasonic nanocrystal surface modification, Fatigue Fract. Eng. Mater. Struct. 32 (2009) Issue 7.
[33] M. Leitner, W. Mössler, A. Putz, M. Stoschka, Effect of post-weld heat treatment on the fatigue strength of HFMI-treated mild steel joints, Weld World 59 (2015) 861–873.
[34] A. Mirzaee-Sisan, Welding residual stresses in a strip of a pipe, Int. J. Press. Vessels Pip. 159 (January 2018) 28–34.
[35] D. Dubois, J. Devaux, J.B. Leblond, Numerical simulation of a welding operation: calculation of residual stresses and hydrogen diffusion, 5th international conference on pressure vessel technology, California, (1984).
[36] A. Mirzaee-Sisan, A. Bastola, Redistribution of welding residual stress following high plastic deformation in seamless pipes, Int. J. Press. Vessels Pip. 158 (2017) 37–50.
[37] A. Hobbacher, Recommendation for fatigue design of welded joints and components, international institute of welding, May 2014.
[38] F. Shen, B. Zhao, L. Li, C. Kai Chua, K. Zhou, Fatigue damage evolution and lifetime prediction of welded joints with the consideration of residual stresses and porosity, Int. J. Fatigue 103 (2017) 272–279.
[39] K. Zhan, C.H. Jiang, V. Ji, Residual stress relaxation of shot peened deformation surface layer on S30432 Austenite steel under applied loading, Japan Instit. Metals, Mater. Trans. 53 (9) (2012) 1578–1581.
[40] C. Rubio-González, A. Garnica-Guzmán, G. Gómez-Rosas, Relaxation of residual stresses induced by laser shock processing, revista Mexica de fisica 55 (4) (2009) 256–261.
[41] N. Tadic, M. Jelic, D. Lucic, M. Misovic, Relaxation of the residual stresses produced by plastic defamation, Mater. Technol. 45 (5) (2011) 467–475.
[42] O. Suliman Zaroog, A. Ali, B.B. Sagari, R. Zahari, Modelling of residual stress relaxation: A review, Pertanika J. Sci. & Technol. 17 (2) (2009) 211–218.
[43] H. Al-Karawi, R.U. Franz von Bock und Polach, M. Al-Emrani, Fatigue crack repair in welded structures via tungsten inert gas remelting and high-frequency mechanical impact, J. Constr. Steel Res. 172 (2020).